Available online at www.sciencedirect.com
SCIENCE DIRECT®
Catalysis Today 87 (2003) 227–235
CATALYSIS TODAY
www.elsevier.com/locate/cattod

Liquid phase methanol reforming with water over silica supported Pt–Ru catalysts

Toshihiro Miyao, Masaya Yamauchi, Shuichi Naito*

Department of Applied Chemistry, Faculty of Engineering, Kanagawa University, 3-27-1, Rokkakubashi, Kanagawa-ku, Yokohama 221-8686, Japan

Abstract

The mechanism of the liquid phase methanol reforming reaction over silica supported Pt–Ru catalyst was investigated by kinetic studies, employing a pyrex glass reactor with reflux condensers connected to a closed gas circulation system under ambient pressure. The rate of H_2 formation over Pt–Ru/SiO_2 catalysts was more than 20 times faster than that over Pt/SiO_2 catalysts with high selectivity for CO_2 (72.3%), indicating a marked addition effect of Ru. In the case of HCHO–H_2O reaction over Pt–Ru/SiO_2, the H_2 formation rate was five times larger than that in the CH_3OH–H_2O reaction but selectivity to CO_2 was only 4%. On the contrary, in the $HCOOCH_3$–H_2O and HCOOH–H_2O reactions, both high activity and selectivity were observed over Pt–Ru/SiO_2. These results clearly indicate that the CO_2 formation does not proceed via HCHO decomposition and following water gas shift reaction. We propose the following pathway for liquid phase methanol reforming reaction over Pt–Ru/SiO_2; a partly dehydrogenated methanol (CH_2OH^*) is the initial reaction intermediate, from which H_2 and CO_2 are formed through $HCOOCH_3$ and HCOOH as the successive reaction intermediates.

Keywords: Liquid phase; Methanol; Pt–Ru

1. Introduction

In recent years liquid phase reforming of methanol with water has attracted great attention because of the requirement to develop more selective hydrogen production process or efficient direct methanol fuel cell. Many investigations have been reported on the liquid phase methanol reforming reaction, but most of them are limited to the studies from an electrochemical viewpoint [1,2]. The most significant issue to be solved for the development of useful high efficiency methanol fuel cells is the insufficient activity of catalysts under the practical conditions and the inhibition of carbon monoxide that was generated during a dehydrogenation of methanol. It has been well accepted that platinum metal possesses the highest activity for the dehydrogenation of methanol, although it is still not enough for practical use. To overcome these problems, several research groups have been investigating the second component addition effect to the platinum catalysts. Among them, Pt–Sn, Pt–Fe, Pt–Ni and Pt–Ru catalysts were reported to show extremely high activities for this reaction [3–5]. At present, the Pt–Ru/C catalyst shows the highest activity for this reaction, where dissociative chemisorption of methanol occurs on Pt surface and the following oxidation of the carbonaceous adsorbate to CO_2 takes place on the surface oxy-species sites formed by the presence of Ru [6,7]. The reaction mechanisms on Pt and Pt–Ru alloy anode catalysts have been studied by

* Corresponding author. Tel.: +81-45-481-5661x3903; fax: +81-45-491-7915.
E-mail address: naitos01@kanagawa-u.ac.jp (S. Naito).

0920-5861/$ – see front matter © 2003 Elsevier B.V. All rights reserved.
doi:10.1016/j.cattod.2003.10.003

in situ FT-IRAS (Fourier transform infrared reflection absorption spectroscopy) technique [8,9], which revealed that the amount of inhibiting adsorbate CO is to a less extent over Pt–Ru alloy catalysts and is more weakly bonded to the surface than over Pt catalysts. But these investigations were performed at room temperature, which was quite different from the practical conditions in the fuel cells.

On the other hand, gas phase steam reforming reactions of methanol have been examined already in detail and supported Cu metal catalysts have been reported to show an excellent catalytic activity [10]. The reaction proceeds through $HCOOCH_3$ intermediates over Cu catalysts whereas through the decomposition of HCHO over group VIII metal catalysts. It is also reported that there exists a marked support effect for the steam reforming reaction over supported group VIII metal catalysts. For example, in the case of supported Pd catalysts, ZnO supported catalyst exhibited extremely high activity because of the formation of PdZn alloys [11]. However, because the investigations of the liquid phase methanol reforming are still limited only for the development of the electrode of DMFC, the researches dealing with non-platinum catalysts or oxide additives are very few [12]. Moreover few researches have been concentrated to elucidate the mechanism of the liquid phase reforming reaction from a viewpoint of catalysis, except the study on a hydrogen evolution from methanol by using homogeneous ruthenium catalysts [13] or the studies of electro-catalytic activity of Pt/TiO_2 for the anodic methanol oxidation [12].

In the present study, we have studied the mechanism of methanol reforming reaction in liquid phase over supported Pt–Ru catalysts by means of kinetical investigation. The effect of Ru-addition to Pt/SiO_2 for the catalytic performance in the reaction was also discussed in depth.

2. Experimental

2.1. Preparation of catalysts

Silica supported Pt, Ru and Pt–Ru catalysts were prepared by a conventional impregnation method. SiO_2 (Japan Aerosil, Aerosil300) was impregnated to an aqueous solution of $H_2PtCl_6{\cdot}6H_2O$ (Wako Pure Chemical), $RuCl_3$ (Wako Pure Chemical) or the mixed solution of both precursors. The amount of metal loading in Pt/SiO_2 and Ru/SiO_2 catalysts were adjusted to 5 wt.%. In $Pt–Ru/SiO_2$ catalyst, the loading of Pt was adjusted to 5 wt.% and the molar ratio of Pt/Ru was unity. The impregnated samples were then evaporated at 308 K and dried overnight at 383 K.

2.2. Procedure of catalytic reactions

The 0.5 g of catalyst was placed in a round bottom reactor (pyrex glass, 300 ml) with reflux condensers connected to a closed gas circulation system, and reduced by hydrogen at 673 K for 5 h. After the catalyst pretreatment in the gas phase, 60 cm^3 of degassed methanol solution (typically 10% CH_3OH/H_2O) was introduced into the reactor under nitrogen atmosphere by using Schlenk technique. The catalyst suspension of methanol solution was further degassed at liquid nitrogen temperature to remove trace amount of air. Then the reactor was heated with an oil bath until the refluxing of the methanol solution started under methanol and water vapor pressures with the balanced nitrogen gas as an internal standard. The reaction rates were mainly measured between 350 and 357 K. Gas phase products were analyzed by TCD gas chromatograph (GC-3BT, Shimadzu) and liquid phase products were analyzed by FID gas chromatograph (GC-14B, Shimadzu).

2.3. Characterization of catalysts

A transmission electron microscope (JEM2010, JEOL) with an acceleration voltage of 200 kV and LaB_6 cathode was applied for the observation of the images of supported catalysts. Samples were prepared by suspending the catalyst powder ultrasonically in 2-propanol and depositing a drop of the suspension on a standard copper grid covered with carbon monolayer film. An X-ray photoelectron spectroscopy (JPS-9010, JEOL) with Mg Kα X-ray source (10 kV, 10 mA) was applied for the analysis of the electronic states of supported catalysts. Samples were prepared by molding in thin disk shape and etched by accelerated Ar ion beam for 30 s. The amount of hydrogen adsorption was measured by a static volumetric adsorption apparatus (Omnisorp100CX, Beckmann Coulter) at room temperature and used for TOF estimation. Before adsorption measurements, used

catalysts were dried at room temperature and reduced at 673 K for 5 h in a flow of hydrogen at atmospheric pressure. The Pt dispersion (*D* (%); percentage of Pt exposed to the surface) on silica support was evaluated from the amount of chemisorbed hydrogen, assuming spherical Pt particles and an adsorption stoichiometry (H_2:surface Pt) of 2:1. The contribution of the ruthenium to a hydrogen adsorption quantity was neglected in the calculation for bimetallic catalysts.

3. Results and discussion

3.1. Methanol reforming reactions in liquid phase over SiO_2 supported Pt, Ru and Pt–Ru catalysts

Fig. 1 shows the time courses of hydrogen formation during methanol liquid phase reforming over Pt/SiO_2, Ru/SiO_2 and $Pt–Ru/SiO_2$ catalysts at 350 K, where H_2, CO_2, CO and methylformate were observed as the products. The hydrogen formation rate over Pt/SiO_2 catalyst was decreased abruptly after 30 min of reaction and reached nearly zero after 300 min. The Ru/SiO_2 catalyst exhibited similar profiles of hydrogen formation with the Pt/SiO_2 catalyst. On the contrary, the $Pt–Ru/SiO_2$ catalyst showed much higher activity compared with these catalysts. Hydrogen was linearly generated for a longer reaction and the amount of hydrogen formed after 300 min was more than 20 times larger (450 μmol during reaction for 300 min) than that over Pt/SiO_2 or Ru/SiO_2 catalyst.

Table 1 summarizes the formation rates and the selectivity of these products over various silica supported catalysts with their metal dispersions determined by H_2 chemisorption at room temperature. The TOF to hydrogen over $Pt–Ru/SiO_2$ was much larger than that over Pt/SiO_2 although the selectivity to CO_2($=CO_2/(CO_2 + CO) \times 100\%$) was almost the same. On the contrary, over Ru/SiO_2 catalyst, the TOF was about a half of that over $Pt–Ru/SiO_2$, while the selectivity to CO_2 was almost zero in the $CH_3OH–H_2O$

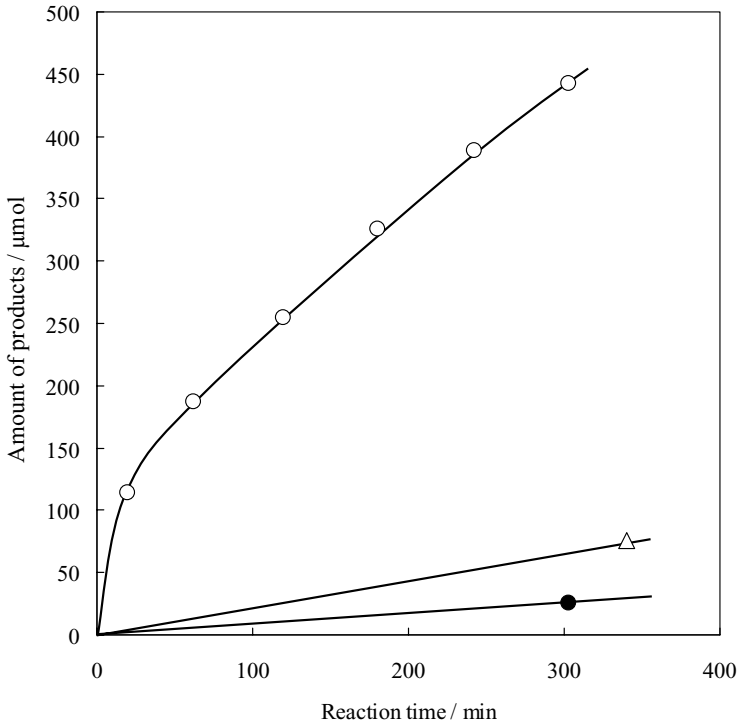

Fig. 1. Liquid phase methanol reforming reaction over 5 wt.% $Pt–Ru/SiO_2$ catalyst at 350 K.

Table 1
Catalytic performance of supported group VIII metal catalysts

Reactant	Catalysts	Formation rate (μmol h^{-1})			TOF (H_2) ($\times 10^{-4}$ s^{-1})	CO_2 (selectivity)	D (%)
		H_2	CO	CO_2			
CH_3OH–H_2O	Pt–Ru/SiO_2	61.6	5.1	13.3	5.57	72.3	24.0
	Pt/SiO_2	3.5	0.2	0.7	0.26	76.5	29.0
	Ru/SiO_2	29.1	27.6	0.0	2.14	0.0	29.5
	Cu/ZnO[a]	0.7	0.8	0.1	–	11.0	–
HCHO–H_2O	Pt–Ru/SiO_2	309.2	397.0	16.4		4.0	
	Pt/SiO_2	12.7	15.5	4.6		23.1	
$HCOOCH_3$–H_2O	Pt–Ru/SiO_2	226.6	72.8	263.7		78.4	
	Pt/SiO_2	57.2	8.6	68.4		88.9	
	Ru/SiO_2	32.5	16.0	3.0		15.7	
HCOOH–H_2O	Pt–Ru/SiO_2	360.6	0.0	431.5		100	
	Pt/SiO_2	64.2	2.1	86.1		97.6	

[a] Commercial catalyst (Süd Chemie).

reaction. On the other hand, the commercial Cu/ZnO reforming catalyst exhibited almost no activity under the same liquid phase reaction condition as Pt based catalysts, although quite high activity was reported to the steam reforming reaction of methanol [10].

3.2. Reaction pathways of the liquid phase reforming over Pt–Ru/SiO_2 catalyst

Takezawa and coworkers [10,14] reported that in the steam reforming reaction, methanol is dehydrogenated to HCHO and $HCOOCH_3$ over copper catalysts, while over group VIII metal catalysts it decomposes to CO and H_2 through the reaction $CH_3OH \rightarrow HCHO + H_2$. They demonstrated that the formation of methylformate from formaldehyde is enhanced by the presence of methanol to an appreciable extent [15]. Also Saito and coworkers [16] reported that the liquid phase methanol reforming reaction over Ni–Ru/C catalyst at 473 K proceeds through formaldehyde as an intermediate. In the present study, it was suggested that the reforming reaction might proceed via dehydrogenation of CH_3OH to $HCOOCH_3$ because considerable amount (210 μmol/6 h) of $HCOOCH_3$ was observed in the liquid phase during the reaction. The carbon mass balance including CO_2, $HCOOCH_3$ and CO was in good agreement with the value calculated from the amount of hydrogen produced.

To clarify the mechanism of liquid phase methanol reforming reaction, the HCHO–H_2O, $HCOOCH_3$–H_2O and HCOOH–H_2O reactions were examined over Pt–Ru/SiO_2 catalyst and compared with the CH_3OH–H_2O reaction. The results are shown in Fig. 2(a)–(d) and summarized in Table 1. In the case of HCHO–H_2O reaction, the H_2 formation rate was five times larger than that in the CH_3OH–H_2O reaction but the selectivity to CO_2 was only 4%. On the contrary, in the $HCOOCH_3$–H_2O and the HCOOH–H_2O reactions, both high activity and selectivity for H_2 and CO_2 were obtained. In addition, in the case of HCHO–CH_3OH–H_2O reaction, the amount of formed methylformate was not affected by the concentration of methanol in the reactant, suggesting that HCHO–H_2O and CH_3OH–H_2O reactions proceed independent of each other. These results clearly indicate that the CO_2 formation does not proceed via HCHO decomposition and the dehydrogenation of methanol to HCHO is a miner side reaction. We suppose that a partly dehydrogenated $[CH_2OH]^*$ may be an intermediate for $HCOOCH_3$ formation, and CO_2 may be formed by its decomposition through HCOOH. The difference of the investigated reaction temperatures in our study may cause the difference from the reaction scheme supposed by Takezawa and Saito. It is thought that at higher temperatures, the intermediate of $[CH_2OH]^*$ is apt to be unstable and dehydrogenated to HCHO.

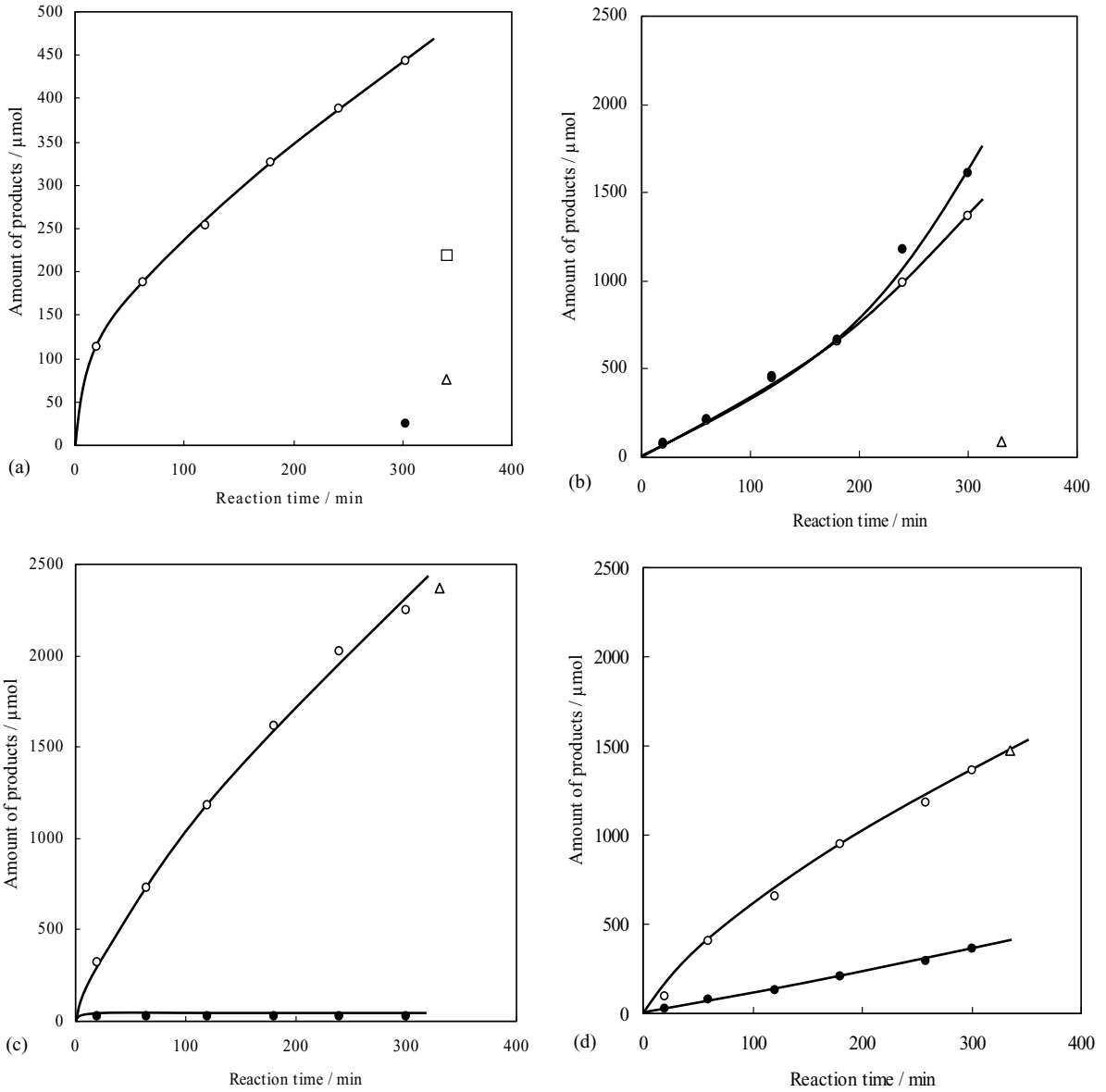

Fig. 2. Time courses of various reforming reactions over 5 wt.% Pt–Ru/SiO_2 catalyst. Reaction temperature: 350 K. (a) CH_3OH–H_2O reaction; (b) HCHO–H_2O reaction; (c) HCOOH–H_2O reaction; (d) $HCOOCH_3$–H_2O reaction. ○: H_2; △: CO_2; □: $HCOOCH_3$; ●: CO.

3.3. *Effect of Ru-addition to Pt/SiO_2 upon the catalytic performance and the morphology*

At present, the enhancement effect of Ru in the Pt–Ru bimetallic catalysts is believed that adsorbed OH(a) formed from water on ruthenium sites may oxidize CO(a) adsorbed on platinum sites more easily than monometallic Pt catalysts [8,17]. In this study, the role of added Ru was investigated for the tolerance effect against CO by adding CO into the gas phase during the methanol reforming reaction over Pt–Ru/SiO_2 catalyst. As shown in Fig. 3 after 145 min

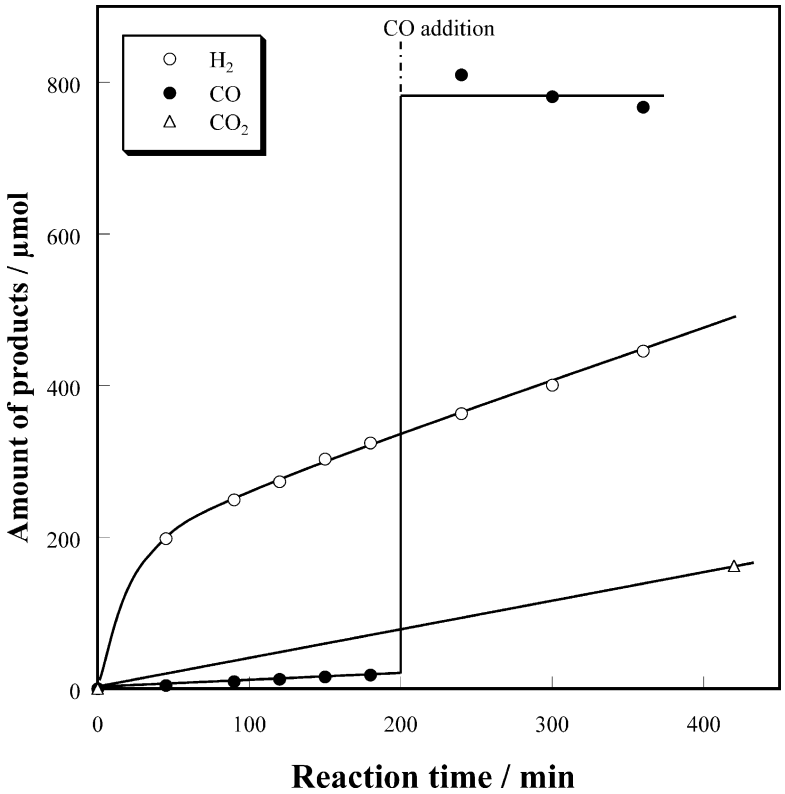

Fig. 3. Effect of CO addition during CH_3OH–H_2O reaction over 5 wt.% Pt–Ru/SiO_2 catalyst at 357 K.

of the CH_3OH–H_2O reaction, 40 Torr of CO gas was added into the gas phase of the reaction system. It was observed that amount of CO in gas phase determined by GC increased immediately to the value corresponding to the amount of added CO, but the rate of hydrogen formation was not affected at all by the added CO. This result indicates that the rate of product formation over Pt–Ru/SiO_2 catalyst is not inhibited by CO in the reactants.

The results of HCHO–H_2O, $HCOOCH_3$–H_2O and HCOOH–H_2O reactions over Pt/SiO_2 and Ru/SiO_2 catalysts were also summarized in Table 1. The Pt/SiO_2 catalyst exhibited relatively large H_2 formation rate in the $HCOOCH_3$–H_2O reaction (57.2 μmol/h) and in the HCOOH–H_2O reaction (64.2 μmol/h), while its activities for the CH_3OH–H_2O reaction and the HCHO–H_2O reaction were poor (3.5 and 12.7 μmol/h of H_2 formation rate, respectively). It is thought that the formed CO may suppress the activity of Pt/SiO_2 catalyst during CH_3OH and HCHO reforming reactions because larger amount of formed CO was formed than the case of $HCOOCH_3$ or HCOOH reaction. The Ru/SiO_2 catalyst exhibited quite different selectivity for CO_2 formation during CH_3OH–H_2O reaction from Pt–Ru/SiO_2 and Pt/SiO_2 catalysts. The reforming reaction over Ru/SiO_2 catalyst may proceed through HCHO intermediate, followed by its decomposition to CO and H_2. Because the catalytic performance of Pt–Ru bimetallic catalyst is quite different from that of Pt or Ru monometallic catalyst, it is thought that the alloying of Pt and Ru plays an extremely important role in the high activity of the Pt–Ru/SiO_2 catalyst.

X-ray diffraction analysis showed that Pt–Ru/SiO_2 catalyst exhibited the diffraction peaks of fcc structure (Fig. 4). An obvious peak shift (0.6°) to higher 2θ value was observed in the diffraction peak of the (1 1 1) reflection in the Pt–Ru/SiO_2 sample ($2\theta = 40.5°$) compared to the Pt/SiO_2 catalyst ($2\theta = 39.9°$). The shift of the observed peak may be caused by the

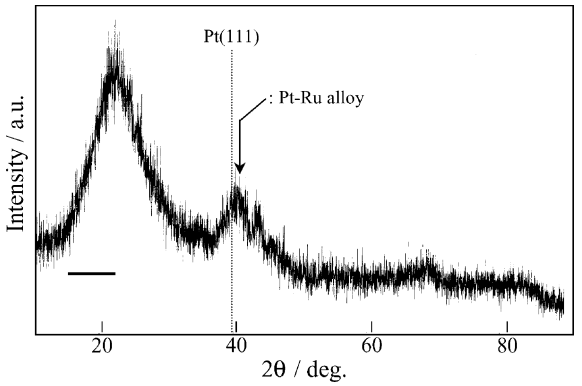

Fig. 4. XRD pattern of 5 wt.% Pt–Ru/SiO_2 (used).

formation of solid solution of Pt and Ru [18]. The TEM image of Pt–Ru/SiO_2 catalyst after the reforming reaction is demonstrated in Fig. 5. A bimodal distribution of dark particles was observed which could be classified into two distinct distributions over 5 nm and under 2 nm particles. The larger particles were assigned to crystallites of Pt and Ru by the energy dispersive X-ray spectroscopy (EDS) analysis, which also supports the formation of solid solution of Pt–Ru metal particles on the silica support. Amount of hydrogen uptake on used catalysts were measured at room temperature. The size of metal particles estimated by the amount of hydrogen adsorption (4.7 nm) is in good agreement with the particle size determined by TEM observation.

The electronic states of surface species in the used Pt–Ru catalyst were investigated by XPS measurements. Fig. 6 shows the Pt_{4f}, Ru_{3d} and Si_{2p} transition spectra for Pt–Ru/SiO_2 catalyst. The Pt_{4f} spectrum of Pt–Ru/SiO_2 catalyst reveals a presence of zerovalent Pt species at 71.4 eV. On the other hand, since $Ru_{3d5/2}$ peak is observed at 280.4 eV, it is suggested that Ru is in an oxidized state. Another peak observed at 284.1 eV is attributed to carbon species formed during the reaction. From the estimation of the peak intensities, it is revealed that the atomic ratio of Pt/Ru on the surface is close to 1 (Pt/Ru = 1.00), which are corrected by the cross-sections of the corresponding ions. These results indicate that surface enrichment of Pt or Ru is not the case of Pt–Ru/SiO_2 catalysts employed in the present study.

Now we are investigating the support effect of Pt–Ru catalysts to develop more efficient catalysts for methanol reforming reaction.

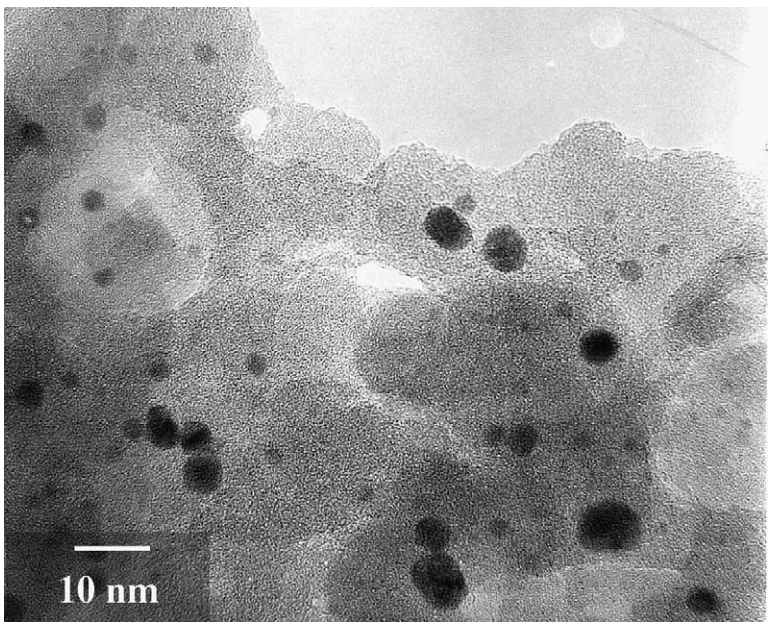

Fig. 5. TEM image of 5 wt.% Pt–Ru/SiO_2 catalyst (used).

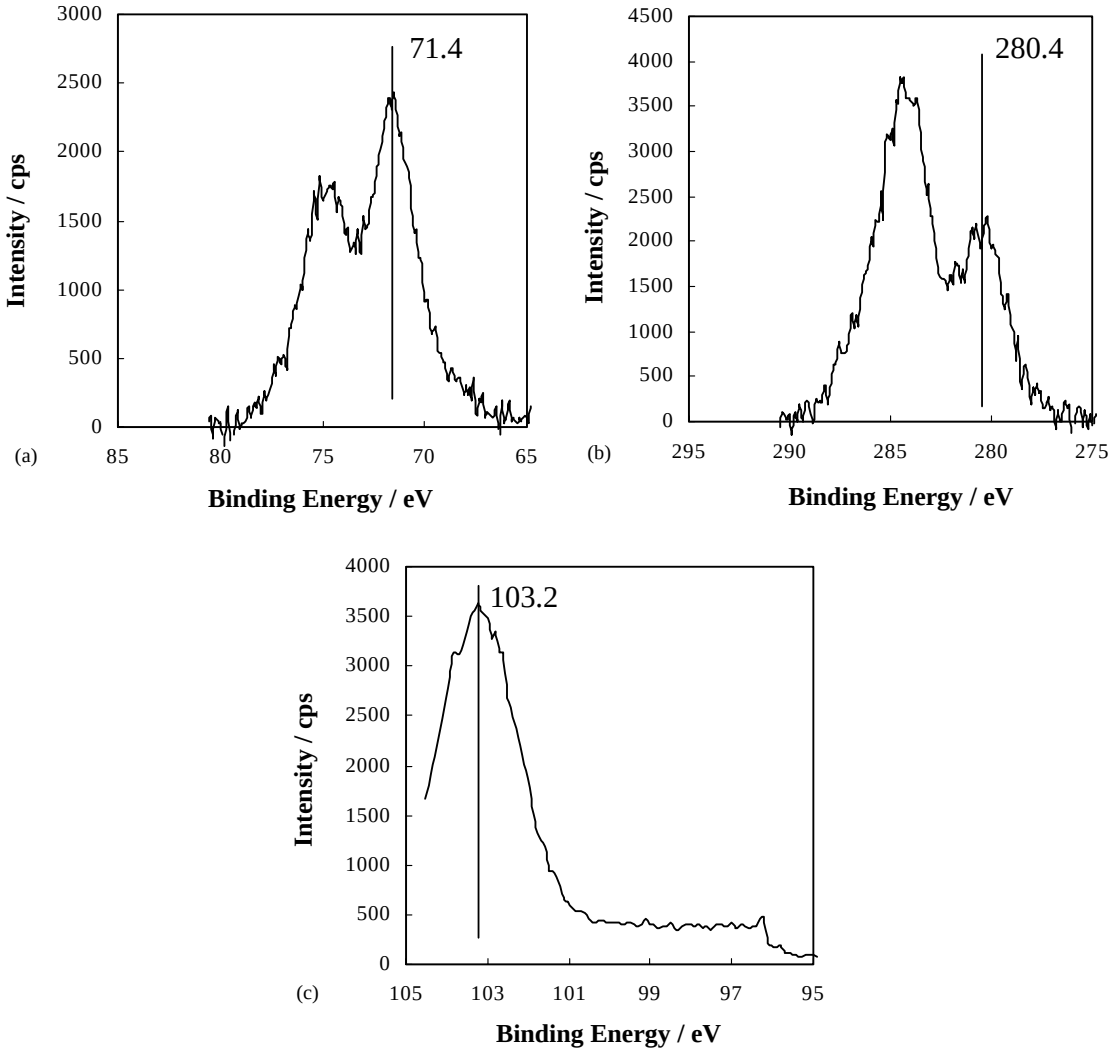

Fig. 6. XPS results of Pt–Ru/SiO_2 catalyst (used): (a) Pt_{4f}; (b) Ru_{3d}; (c) Si_{2p}.

4. Conclusion

In the methanol reforming reaction, Pt–Ru/SiO_2 catalyst exhibited much higher activity than Pt/SiO_2 and Ru/SiO_2 catalysts. The formation of solid solution of Pt and Ru by the addition of Ru to the Pt/SiO_2 catalyst improved a CO tolerance capacity remarkably. The reforming reaction over Pt–Ru/SiO_2 catalyst proceeded through $HCOOCH_3$ and HCOOH and the CO_2 formation did not proceed via HCHO decomposition. The dehydrogenation of methanol is the rate determining step of the reaction.

Acknowledgements

This work was financially supported by High-Tech Research Center Project from the Ministry of Education Science, Sports and Culture.

References

[1] A.B. Anderson, E. Grantscharova, S. Seong, J. Electrochem. Soc. 143 (1996) 2075.
[2] H.A. Gasteiger, N. Markovic, P.N. Ross, E.J. Cairns, J. Phys. Chem. 98 (1994) 617.

[3] M. Watanabe, T. Suzuki, S. Motoo, Denki Kagaku 40 (1972) 210.
[4] A. Hammett, B. Kennedy, S. Weeks, J. Electroanal. Chem. 240 (1988) 349.
[5] J. Sobkowski, K. Franaszczuk, A. Piasecki, J. Electroanal. Chem. 196 (1985) 145.
[6] H. Igarashi, T. Fujino, M. Watanabe, Phys. Chem. Chem. Phys. 3 (2001) 306.
[7] S. Wasmus, A. Kuver, J. Electroanal. Chem. 461 (1999) 14.
[8] T. Iwashita, F.C. Nart, W. Vielstich, Ber. Bunsenges. Phys. Chem. 94 (1990) 1030.
[9] I.T. Bae, T. Sasaki, D. Scherson, J. Electroanal. Chem. 297 (1991) 185.
[10] K. Takahashi, H. Kobayashi, N. Takezawa, Chem. Lett. 759 (1985).
[11] N. Takezawa, N. Iwasa, Catal. Today 36 (1997) 45.
[12] J. Otomo, Y. Kondo, C. Wen, K. Eguchi, K. Yamada, H. Takahashi, J. School Eng. The Univ. Tokyo 47 (2000) 29.
[13] T. Fujii, Y. Saito, J. Mol. Catal. 67 (1991) 185.
[14] K. Takahashi, N. Takezawa, H. Kobayashi, Appl. Catal. 2 (1982) 363.
[15] K. Takahashi, N. Takezawa, H. Kobayashi, Chem. Lett. 1061 (1983).
[16] Y. Yatabe, H. Tajima, Y. Saito, Suiso Energy Syst. 25 (2000) 56.
[17] B. Beden, C. Lamy, A. Bewick, K. Kunimatsu, J. Electroanal. Chem. 121 (1981) 343.
[18] A. Arico, P. Creti, P. Antonucci, J. Cho, H. Kim, V. Antonucci, Electrochim. Acta 43 (1998) 3719.